

Electronic Supplementary Information

**Plasmonic hot carrier-driven oxygen evolution reaction on Au
nanoparticles/TiO₂ nanotube arrays**

Song Yi Moon^{a,b}, Hee Chan Song^{b,c}, Eun Heui Gwag^{b,c}, Ievgen I. Nedrygailov^b,

Changhwan Lee^{b,c}, Jeong Jin Kim^b, Won Hui Doh^b and Jeong Young Park^{*,a,b,c}

^a Department of Chemistry, Korea Advanced Institute of Science and Technology (KAIST),
Daejeon 34141, Republic of Korea

^b Center for Nanomaterials and Chemical Reactions, Institute for Basic Science (IBS),
Daejeon 34141, Republic of Korea

^c Graduate School of EEMS, Korea Advanced Institute of Science and Technology (KAIST),
Daejeon 34141, Republic of Korea

*To whom correspondence should be addressed. E-mail: jeongypark@kaist.ac.kr

KEYWORDS: surface plasmon resonance, hot electron, Schottky barrier, oxygen evolution reaction, solar water splitting, nanostructure

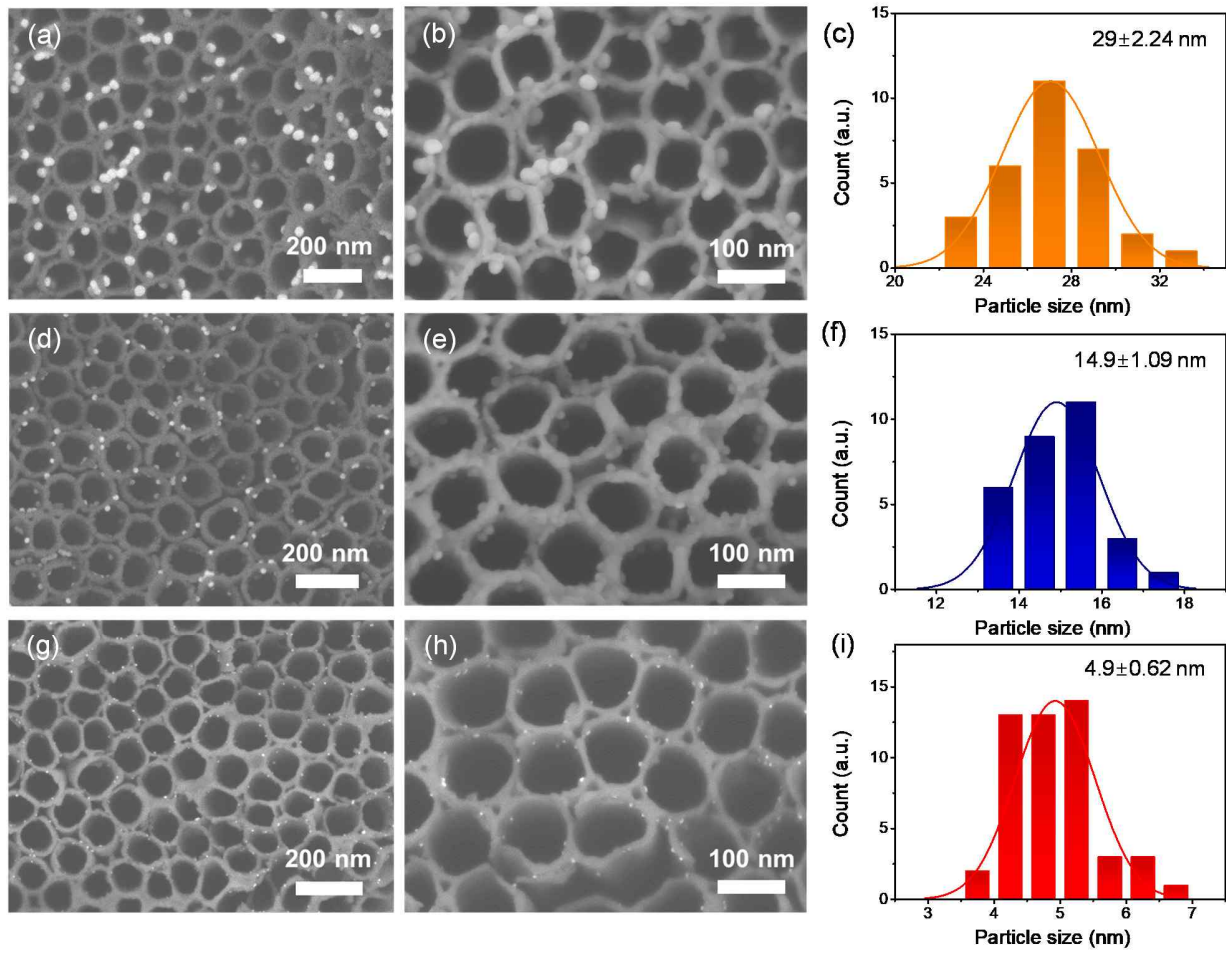


Figure S1. Au particle size distributions on the titania nanotube arrays (TNAs). Scanning electron microscopy images and corresponding histograms showing the size distributions of the Au nanoparticles (NPs) on the surface of the TNAs for (a,b,c) 29 nm Au NPs, (d,e,f) 14.9 nm Au NPs, and (g,h,i) 4.9 nm Au NPs.

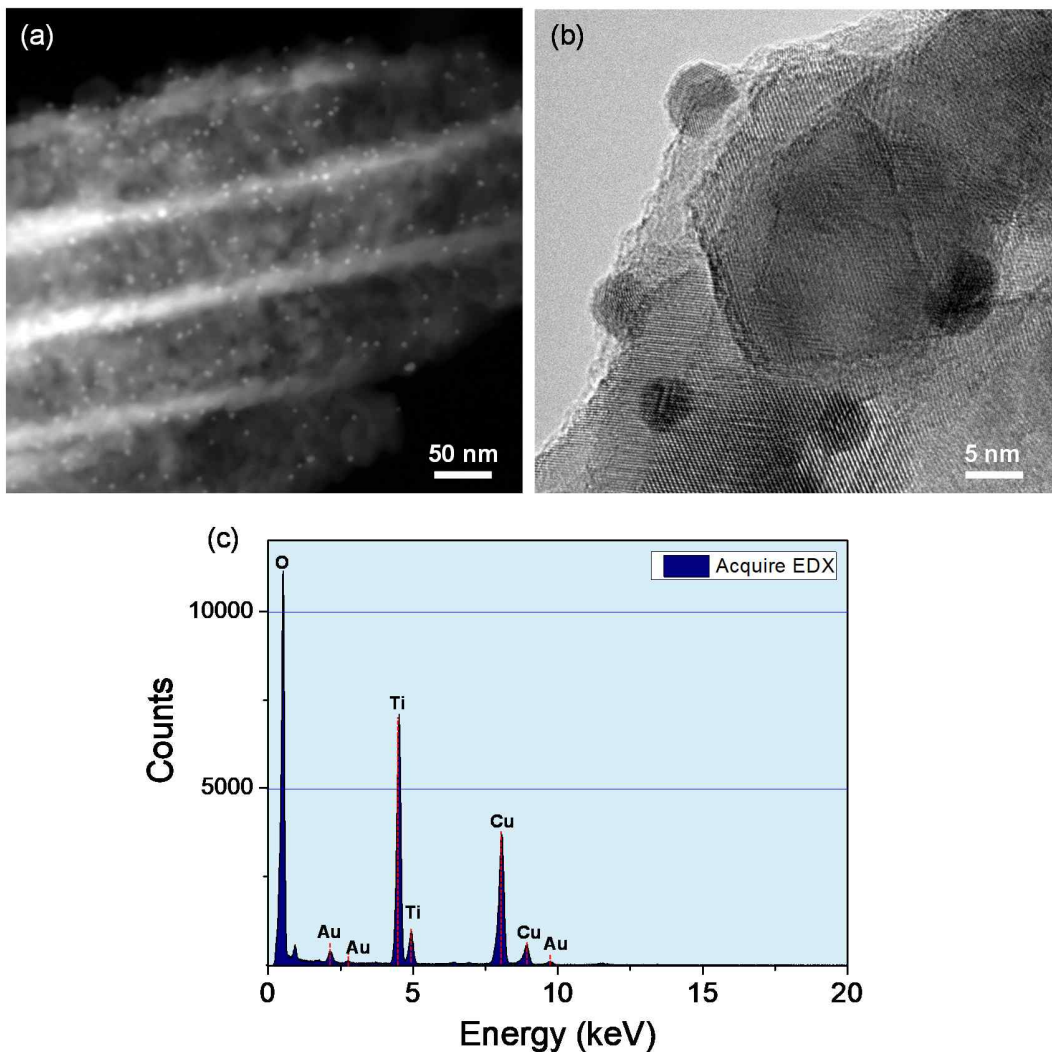


Figure S2. (a) High-angle annular dark-field scanning transmission electron microscope (HAADF-STEM) image showing the 5 nm Au NPs@TNAs. (b) High-resolution transmission electron microscope (HRTEM) image obtained at the interface between the Au NPs and the TiO_2 . (c) Energy dispersive spectroscopy (EDS) spectrum of a 5 nm Au NPs@TNAs (2.67 wt%) sample showing the presence of Au.

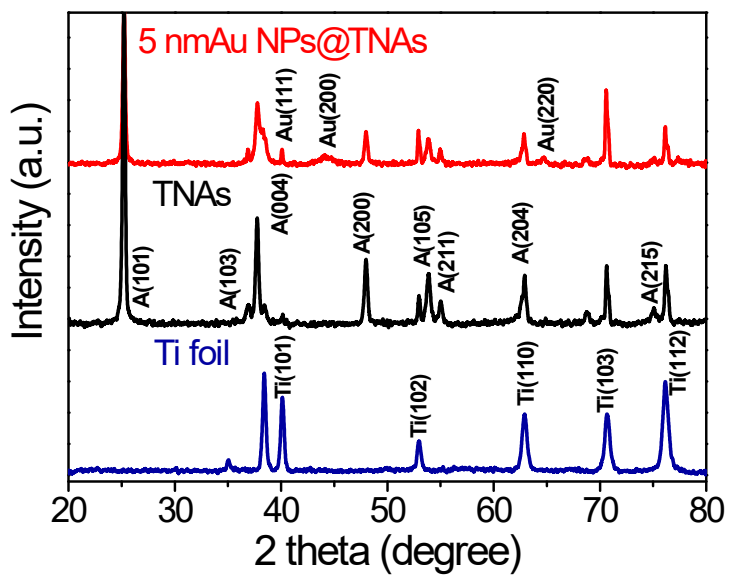


Figure S3. X-ray diffraction (XRD) patterns for the 5 nm Au NPs@TNAs. The XRD pattern for Ti foil is also shown for reference.

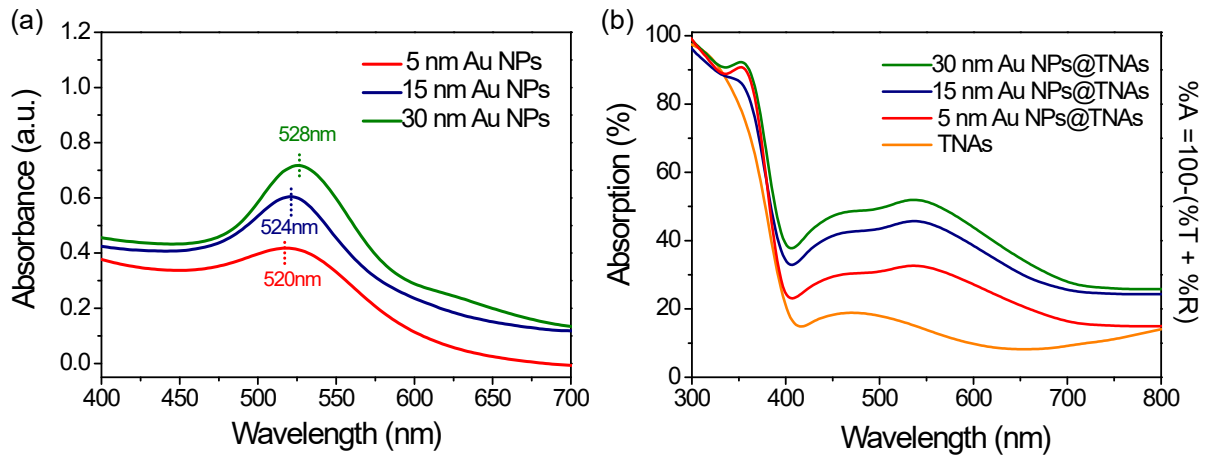


Figure S4. Optical properties of the Au NPs@TNAs. (a) UV–vis absorption spectra of the Au nanoparticles. (b) UV–vis absorption spectra of the 5, 15, and 30 nm Au NPs@TNAs calculated using the relation $\%A = 100 - (\%T + \%R)$.

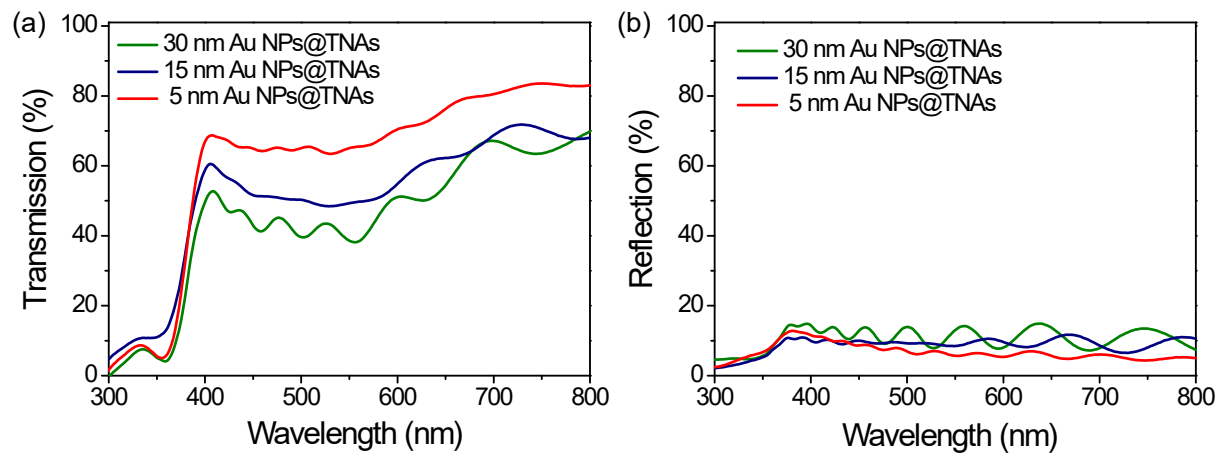


Figure S5. Optical properties of the Au NPs@TNAs. (a) Transmission spectra and (b) UV-vis absorption spectra of the 5, 15, and 30 nm Au NPs@TNAs.

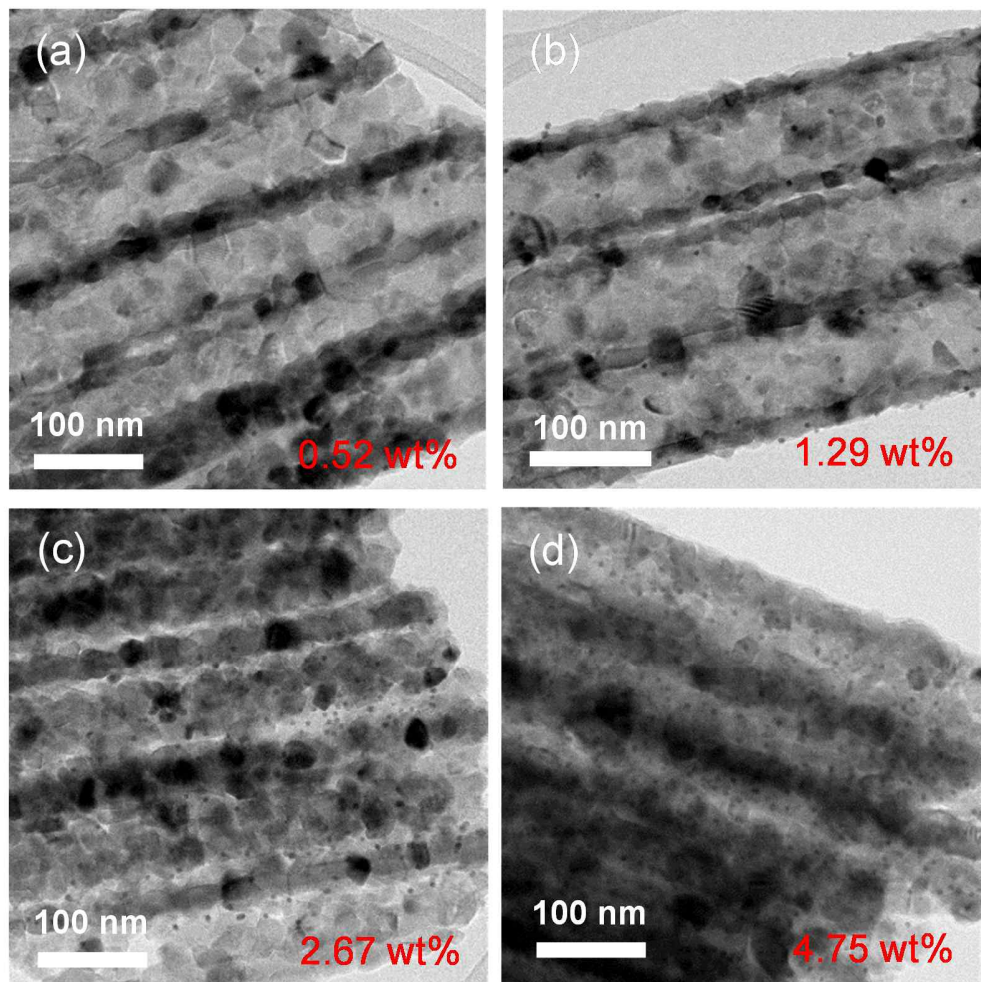


Figure S6. TEM characterization with Au loading dependence. TEM images of the 5 nm Au NPs@TNAs electrode with gold loading between 0.52 and 4.75 wt%.

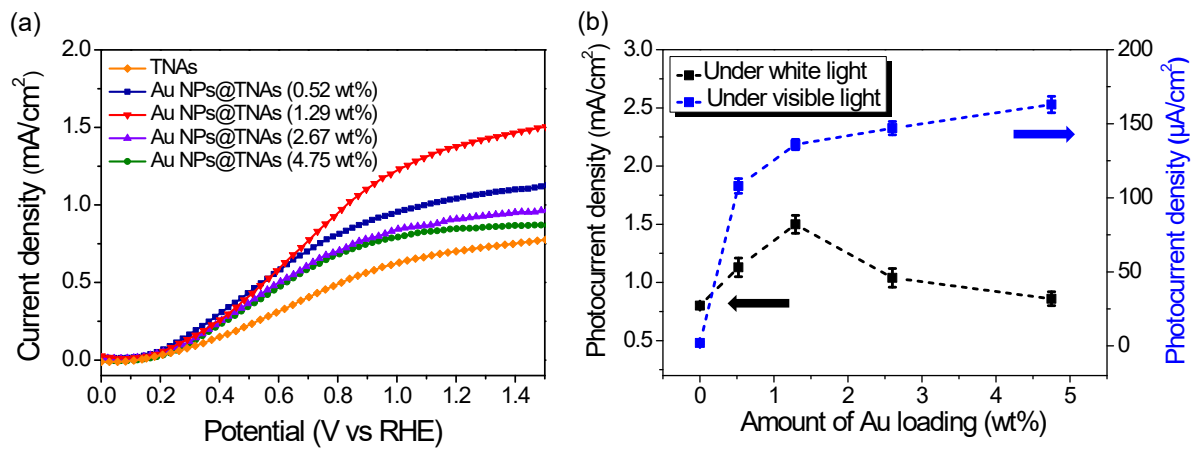


Figure S7. Photoelectrochemical performance with the optimum loading amount of Au. (a) Linear sweep voltammetry of the Au NPs@TNAs electrodes with different gold loading under white light illumination. (b) Photocurrent density as a function of gold loading for the Au NPs@TNAs electrodes under white and visible light illumination.

Calculation of Decay Lifetime. The decay lifetime can be calculated by fitting the V–t curves to a biexponential function $y(t) = A_0 + A_1 e^{-t/\tau_1} + A_2 e^{-t/\tau_2}$ and the harmonic mean of the lifetime (τ_m) is obtained by $\tau_m = (\tau_1 \tau_2) / (\tau_1 + \tau_2)$. Finally, the total lifetimes estimated by $\log(2) \times \tau_m$ of the bare TNAs, 30 nm Au NPs@TNAs, 15 nm Au NPs@TNAs, and 5 nm Au NPs@TNAs are 0.68, 0.63, 0.49, and 0.27 s, respectively.

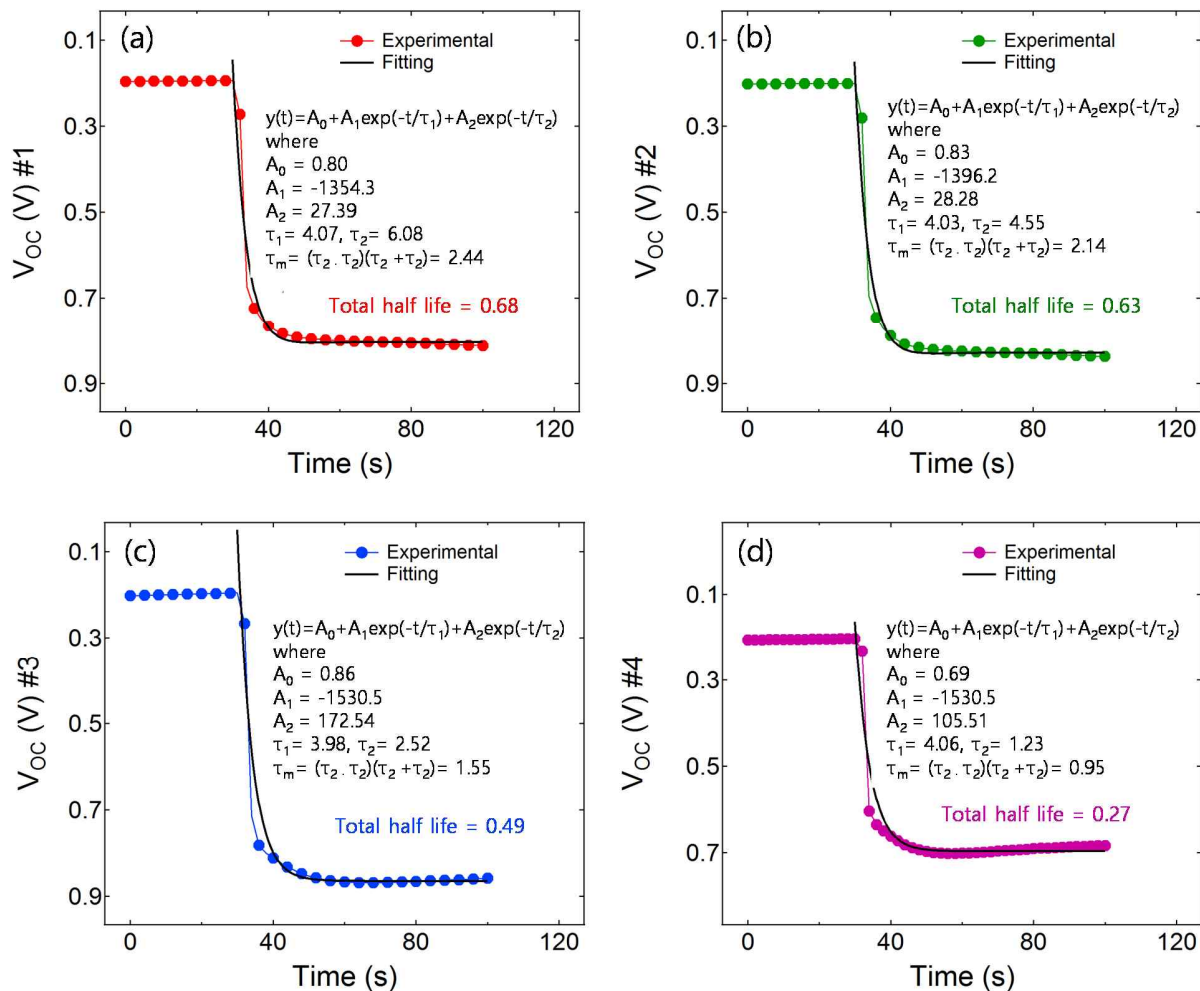


Figure S8. Photovoltage–time spectra collected for (a) bare TNAs and (b) 30nm Au NPs@TNAs, (c) 15nm Au NPs@TNAs, and (d) 5nm Au NPs@TNAs.

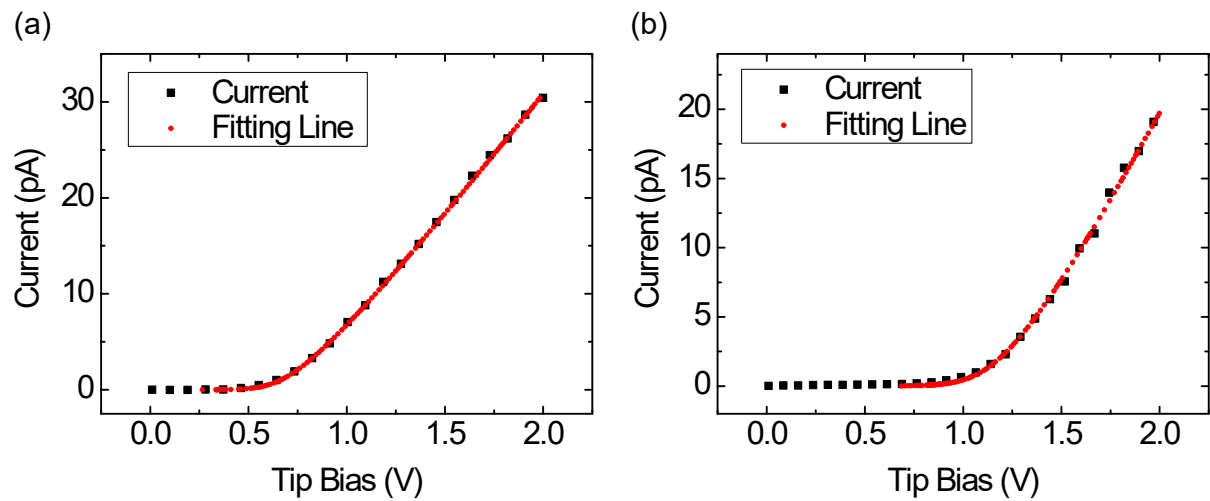


Figure S9. Calculation of the Schottky barrier height. Fitting of the experimental current–voltage curves to the thermionic emission equation for (a) 40 nm Au NPs@TNAs and (b) 76 nm Au NPs@TNAs.

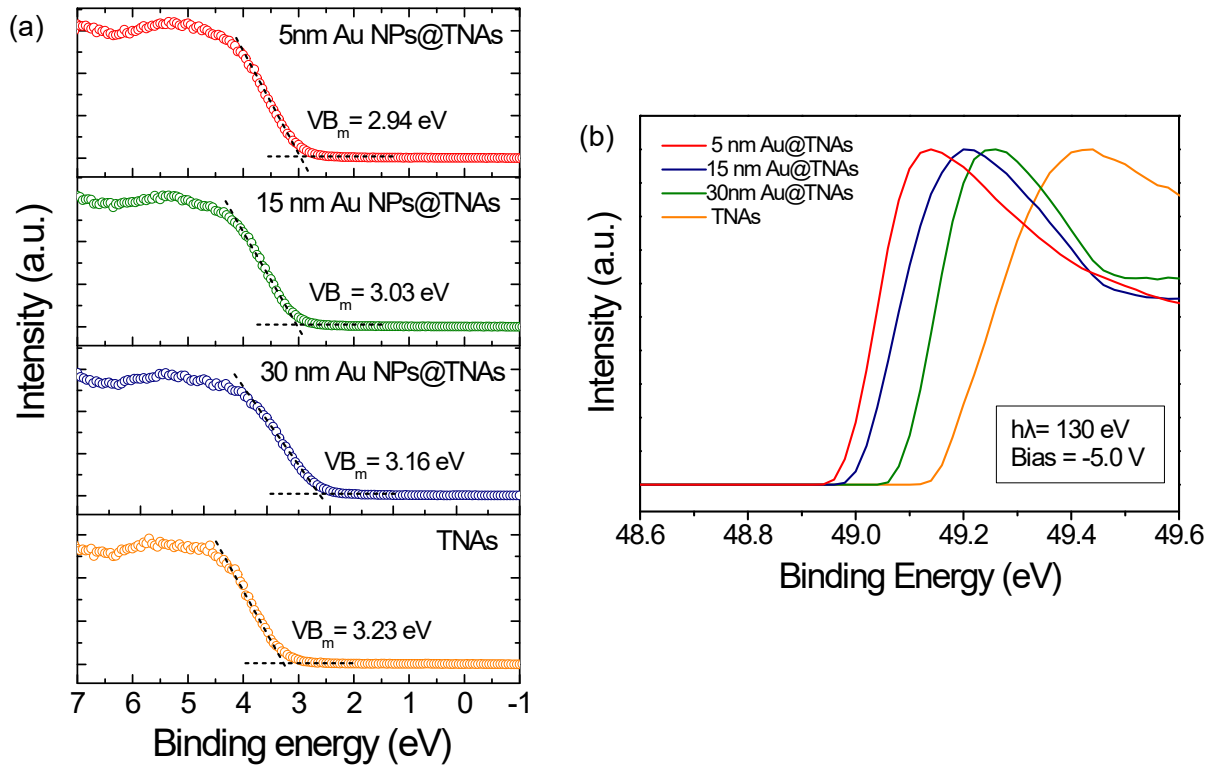


Figure S10. Ultraviolet photoelectron spectroscopy (UPS) spectra. (a) Valence band edges from the Au NPs@TNAs. (b) Secondary electron emission spectra observed for 130 eV photons incident on the Au NPs@TNAs.

Finite-Difference Time-Domain (FDTD) Simulation. The FDTD simulation model was based on TEM images (Figure S2). All the simulations were carried out in three spatial dimensions that are periodic in the x- and y-directions and the perfectly matched layer (PML) was used in the z-direction. The incident light was a plane wave at 537 nm, which is the wavelength of the strongest LSPR excitation.

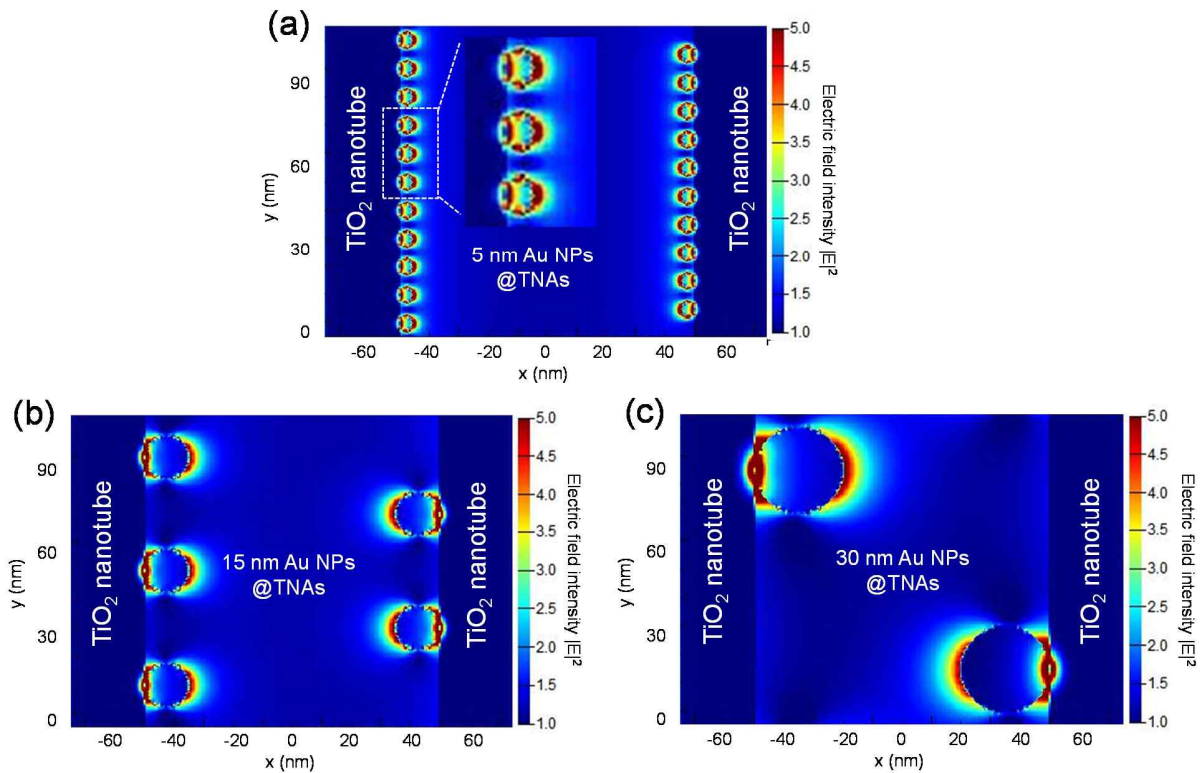


Figure S11. Electric field distribution formed at the Au NPs@TNAs. The gold nanoparticle sizes are (a) 5, (b) 15, and (c) 30 nm. The field images are a cross-section of the Au NPs@TNAs and are output from the FDTD simulation.

Table S1. Atomic weight percentage of Au in the EDX and XPS spectra.

Au wt % on TiO ₂	30 nm Au NPs @TNAs	15 nm Au NPs @TNAs	5 nm Au NPs @TNAs
EDX - Au (L) %	12.095±0.40	3.761±0.14	1.294±0.25
XPS - Au (4f) %	14.863±0.85	4.367±0.43	1.49±0.16

(Amount of Au loading was analyzed at several different spots in the sample)

Table S2. Parameters obtained from fitting the thermionic emission equation to current–voltage (I–V) curves measured on the plasmonic Au NPs@TNAs.

Au NPs diameter (nm)	SBH (φ_b)	Ideal factor (η)
20	0.565 eV	11.9
23	0.52 eV	12
25	0.579 eV	9.2
31	0.571 eV	7.5
35	0.577 eV	7.8
40	0.593 eV	6.32
49	0.64 eV	5.07
58	0.70 eV	4.3
60	0.715 eV	3.7
70	0.73 eV	3.8
75	0.76 eV	2.5